Journal of Catalysis **197,** 335–343 (2001)
doi:10.1006/jcat.2000.3083, available online at http://www.idealibrary.com on IDEAL®

Hydrogenation of Toluene over γ-Al_2O_3-Supported Pt, Pd, and Pd–Pt Model Catalysts Obtained by Laser Vaporization of Bulk Metals

J. L. Rousset,*,[1] L. Stievano,* F. J. Cadete Santos Aires,* C. Geantet,* A. J. Renouprez,* and M. Pellarin†

*Institut de Recherches sur la Catalyse, 2 Av. A. Einstein, 69626 Villeurbanne Cedex, France; and †Laboratoire de Spectrométrie Ionique et Moléculaire, Université Claude Bernard Lyon I, 43 Bd. du 11 Nov 1918, 69622 Villeurbanne Cedex, France

Received July 24, 2000; revised September 18, 2000; accepted September 18, 2000; published online December 21, 2000

Pure Pd, Pt, and bimetallic Pd–Pt clusters produced by laser vaporization of bulk metals or alloys have been deposited on a high surface area alumina (γ-Al_2O_3). The bimetallic clusters have a perfectly well-defined stoichiometry, as demonstrated by energy-dispersive X-ray analysis experiments. Transmission electron microscopy shows that pure or bimetallic clusters have similar size distributions. The catalytic properties of Pd, Pt, $Pd_{17}Pt_{83}$, and $Pd_{65}Pt_{35}$ supported clusters have been investigated in the vapor-phase toluene hydrogenation over a wide range of reaction conditions. The activation energies are 44 $\pm$ 6 kJ/mol. The pressure dependence on toluene varies from 0 at 333 K to 0.7 at 500 K whereas this dependence on H_2 increases from approximately 0.5 at 333 K up to 2.2 at 500 K. The results obtained with the pure metals corroborate those reported in the literature for catalysts prepared by chemical methods. The activities of the bimetallic catalysts do not show any synergy between Pd and Pt but rather a perfect additivity of their individual catalytic properties. Pt has been shown to have no electronic influence on the reactivity of Pd atoms. The nonlinear variation of the turnover frequency as a function of the Pd surface concentration is interpreted on the basis of an active site composed of a pair of atoms.

Key Words: **bimetallic Pd–Pt; laser vaporization; model catalysts; toluene hydrogenation.**

INTRODUCTION

Supported metal catalysts modified by addition of a second metal may substantially differ in terms of activity or selectivity from their monometallic counterparts (1). The final goal of catalytic studies with alloy catalysts is to learn about the functioning of metals and to rationally design catalysts with improved catalytic properties. Bimetallic catalysts based on the association of palladium and platinum have been extensively studied. On one hand, Koussathana *et al.* (2) found that bimetallic Pd–Pt formulations exhibit higher activities than the two pure metals toward the hydrogenation of naphthalene and biphenyl. This enhancement of activity was found to depend on the support. Blomsma *et al.* (3) reported that zeolite-supported Pd–Pt bimetallic bifunctional catalysts are more active and selective in the isomerization of heptane than pure Pt or Pd also supported on zeolite. The Pd–Pt system was also studied by Carturan *et al.* (4) as a function of the Pd/Pt ratio. They reported that in the styrene hydrogenation, the activity of the bimetallic system displays a remarkable increase up to 30% of Pt whereas in the range 30–100% Pt, the activity is simply the sum of the individual activities.

On the other hand, Deganello and co-workers (5) observed that the addition of Pt reduces both the activity and the selectivity of the Pd catalysts in the liquid-phase hydrogenation of 1,3-cyclooctadiene to cyclooctene. In the case of the hydrogenation of phenylacetylene to styrene, Carturan *et al.* (4) found that the specific activity of PdPt catalysts is smaller than the sum of individual Pd and Pt in the 10–100% Pt range.

Other studies have focused on the sulfur tolerance of Pd–Pt alloy deposited on different supports such as Al_2O_3 (6), SiO_2–Al_2O_3 (7, 8), Al_2O_3–B_2O_3 (9), or HY zeolite (10). Industrial applications for hydrogenating aromatics and olefins in hydrocarbon feedstocks on such Pd–Pt alloys were proposed and actually used in plants (11–14). This high sulfur resistance, greatly enhanced by using acidic supports, is often believed to arise from the formation of electron-deficient metal particles.

Since the size, the structure, or the composition of supported bimetallics is difficult to control for active phases obtained by chemical methods, it is generally not straightforward to compare the catalytic properties of a bimetallic catalyst to those of a monometallic one. To make the comparison easier, one needs to prepare monometallic and bimetallic systems having approximately the same size, morphology, and overall, uniform and well-defined composition. The purpose of this paper is to show that all these criteria are fulfilled by using the laser vaporization technique.

In this paper, we report on the preparation, the characterization, and the catalytic behavior of pure Pd or Pt as well

[1] To whom correspondence should be addressed. Fax (00) 04 72 44 53 99. E-mail: rousset@catalyse.univ-lyon1.fr.

0021-9517/01 $35.00

as bimetallic Pd–Pt clusters produced by laser vaporization of bulk metals and alloys and deposited on high surface area alumina (γ-Al_2O_3). The laser vaporization technique allows the generation of ligand-free metal clusters and, in the case of bimetallic systems, particles which all have a composition identical to that of the vaporized alloyed target.

The vapor-phase hydrogenation of toluene has been used to test our catalysts since this reaction has been extensively studied by the group of Vannice over monometallic Pd/Al_2O_3 (15) and Pt/Al_2O_3 (16) catalysts prepared by the incipient wetness technique.

TABLE 1

Mean Diameters of Supported Clusters and Metal Loading of the Catalysts As Deduced Respectively from TEM Experiments and Chemical Analysis

Sample	Metal content (wt%)	Mean diameter (nm)	
		Fresh sample	After annealing
Pd_{100}	0.05	4.0	6.3
$Pd_{65}Pt_{35}$	0.08	3.6	5.2
$Pd_{17}Pt_{83}$	0.07	3.4	5.0
Pt_{100}	0.06	3.4	4.8

EXPERIMENTAL

Catalyst Preparation by Using Low-Energy Cluster Beam Deposition

The laser vaporization cluster source has been extensively described elsewhere (17). The second harmonic of a Nd:YAG pulsed laser is used to vaporize the metal from a rod to create a plasma. Cluster nucleation and growth occur when a continuous flux of inert gas (a mixture of He and Ar) is introduced into the chamber. Differential pumping extraction of the clusters through a skimmer yields a cluster beam which carries neutral and ionized species. The ionized clusters can be analyzed by time-of-flight mass spectrometry (TOFMS). After removal of the ionized clusters by electrostatic deflection, the neutral clusters are deposited on the substrates. Typical deposition rates (equivalent thicknesses) of about 5 nm/min are obtained with neutral clusters of various materials. The deposition rates were monitored using a quartz microbalance. To deposit the clusters on the support, which in the present case is a γ-alumina powder (Condea, Puralox SCFa-240 with a specific area of 240 m^2/g), a device was developed which stirs the power in front of the cluster beam. This device is expected to favor homogeneous cluster deposition on most of the powder grains. After deposition, the samples are air transferred, characterized, and/or used for catalytic reactions. For these experiments, Pd and Pt rods of 99.99 and 99.95% purity, respectively, as well as $Pd_{17}Pt_{83}$ and $Pd_{65}Pt_{35}$ bimetallic rods obtained by melting Pd (99.99% purity) and Pt (99.95% purity) were used. Three grams of Pd, Pt, $Pd_{17}Pt_{83}$, and $Pd_{65}Pt_{35}$ γ-alumina-supported catalysts was prepared. Chemical analysis revealed the metal content of each catalyst, and the corresponding metal loading values are reported in Table 1.

Catalyst Characterization

The morphologic characterization of the supported clusters was performed with a JEOL JEM 2010-F transmission electron microscope (TEM) operating at 200 kV and equipped with a field emission gun (FEG), a high-resolution UHR pole piece (point resolution: 0.196 nm). The composition analysis of the bimetallic systems was done by energy-dispersive X-ray spectroscopy (EDX) with a Pentafet-Link ISIS EDX spectrometer from Oxford Instruments in the TEM.

To obtain suitable samples for TEM characterization, the as-obtained powders were dispersed in ethanol by ultrasonication. A drop of the solution was then deposited onto a thin holey-carbon film supported on a copper microscopy grid (200 mesh, 3.05 mm) and left to dry. The grains of powder containing the metallic particles are well separated and may thus be characterized by TEM.

The determination of the size of the clusters and their distribution over the supports was performed by TEM imaging. Sufficiently intense condensed probes (0.5–2.4 nm) can be obtained with the FEG, which allows EDX-S analysis of very reduced volumes and thus of individual nanometer-size particles. This was performed to verify the chemical homogeneity of the deposited clusters. Large-scale (>20 nm) EDX-S analysis of more or less large collections of particles was also performed by defocusing the electron probe to the required size.

Catalytic Activity Measurements: Toluene Hydrogenation

The hydrogenation of toluene was carried out in a fixed-bed gas-flow microreactor at a constant pressure of 760 Torr (1 atm) between 350 and 540 K. The partial pressure of toluene (Fluka, purity >99%) was varied between 5 and 40 Torr by using a gas-phase saturator system. The partial pressure of H_2 was controlled by dilution with N_2 and the gas flow rates were measured by mass flow meters (Brooks, 0–200 cm^3/min). Toluene and methylcyclohexane, which were the only products detected, were analyzed with an in-line gas chromatograph equipped with a flame ionization detector. The amount of catalyst, which was about 500 mg for each experiment, and the flow rates were chosen to obtain a conversion below 10%, at which a differential model for the determination of the specific rates of reaction can be applied. Prior to the first activity measurement,

each catalyst was pretreated at 573 K for 2 h under hydrogen.

For each data point, a bracketing technique was employed (18), which consisted of 30 min for the system to reach the steady state, 30 min to perform several sample analyses, and again 30 min under pure H_2 for the regeneration of the catalyst, which actually recovers its former activity. During the regeneration, the setup was adjusted to the reaction conditions for the next data point. At the end of the data collection under a range of reaction conditions, several experimental points were repeated to check for the possible deactivation of the catalyst, which was always found to be negligible.

RESULTS

Transmission Electron Microscopy Experiments

Microscopy experiments were performed on each catalyst at three different stages: (1) fresh samples, (2) pretreated samples heated for 2 h at 573 K under hydrogen flow, and (3) after reaction. The photographs for stages 1 and 3 are displayed respectively in Figs. 1 and 2 for $Pd_{17}Pt_{83}$ and pure Pt samples. The size histograms, i.e., before and after reaction, are presented respectively in Figs. 3 and 4. The mean size and standard deviation for all the fresh samples was found to be nearly identical (Table 1). This indicates that the vaporization source produces clusters of the same size whatever the metals or alloys. This has been already checked for other systems such as, for example, Au, Ni, and AuNi clusters (19). After reaction, TEM (Fig. 2) shows that the crystallites have a mean diameter larger than that of the fresh catalysts (Table 1). However, this diameter is identical to that observed for the preheated samples before reaction. Since the catalytic properties of the catalysts do not vary appreciably during the catalytic test, one can deduce that the observed increase of the mean particle size has already occurred during the annealing treatment and not during the reaction. Later on, the structure of the catalysts does not undergo any further change. Energy-dispersive

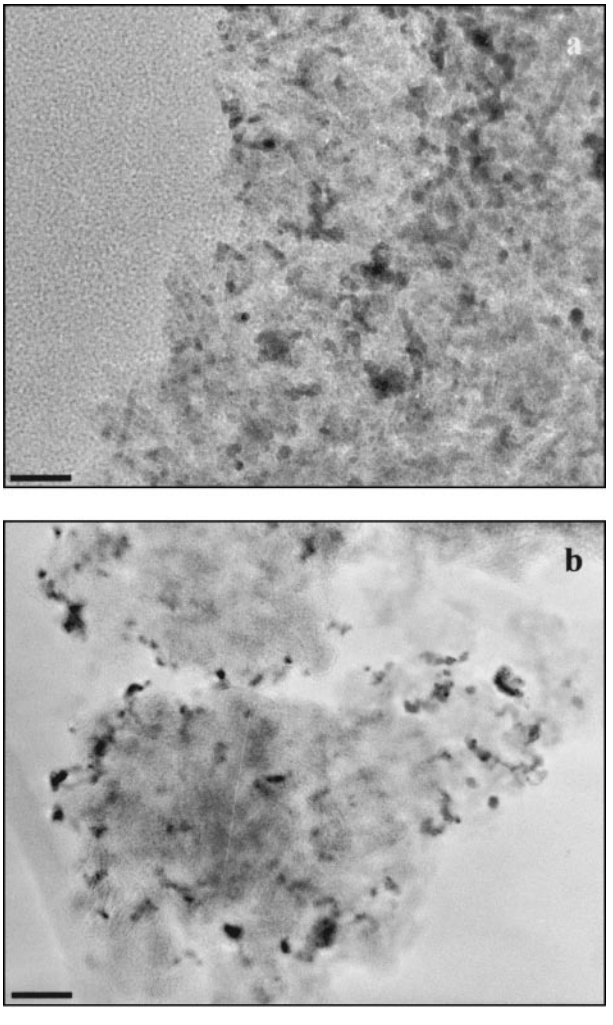

FIG. 1. TEM images of the $Pd_{17}Pt_{83}$ (a) and Pt (b) clusters as deposited on γ-alumina. Scale bars are 20 nm.

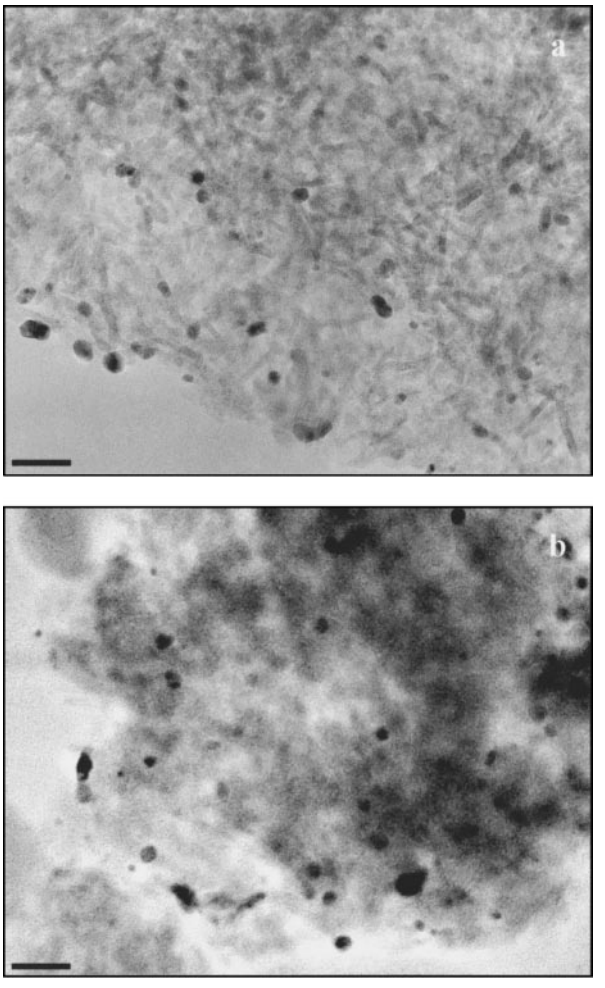

FIG. 2. TEM images of the $Pd_{17}Pt_{83}/Al_2O_3$ (a) and Pt/Al_2O_3 (b) catalysts after reaction. Scale bars are 20 nm.

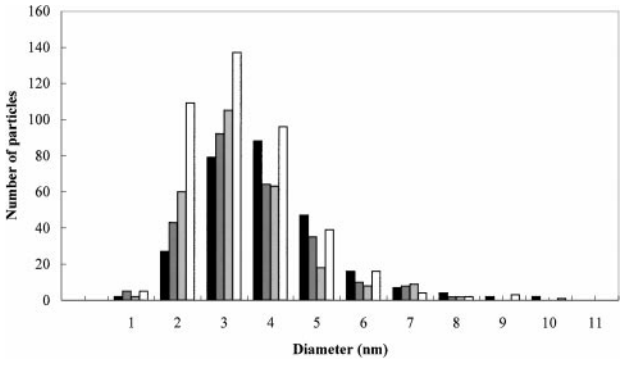

FIG. 3. Size distribution histograms of Pd–Pt clusters as deposited on γ-alumina. Pure Pd (black), $Pd_{65}Pt_{35}$ (dark gray), $Pd_{17}Pt_{83}$ (light gray), and pure Pt (white).

X-ray analysis was used to study the composition of individual particles by defocusing the 1-nm^2 probe to the size of each analyzed cluster for both $Pd_{17}Pt_{83}$ and $Pd_{65}Pt_{35}$ bimetallic samples. Consequently, for both systems, the composition homogeneity was checked and found to be equal to that of the vaporized rod. Figure 5 shows the composition corresponding to the analysis of supported particles for both alloys.

Toluene Hydrogenation

At temperatures below 430 K, the reaction rates measured for all samples lead to linear Arrhenius plots (Fig. 6). The activation energies deduced from these plots in this temperature range are listed in Table 2. The activation energies corresponding to pure Pd and Pt are consistent with those measured on samples prepared by chemical methods (15, 16).

As the temperature is increased, the activity of these catalysts passes through a reversible maximum (Fig. 7). The turnover frequencies (TOF) based on surface metallic atoms were deduced from TEM experiments and size

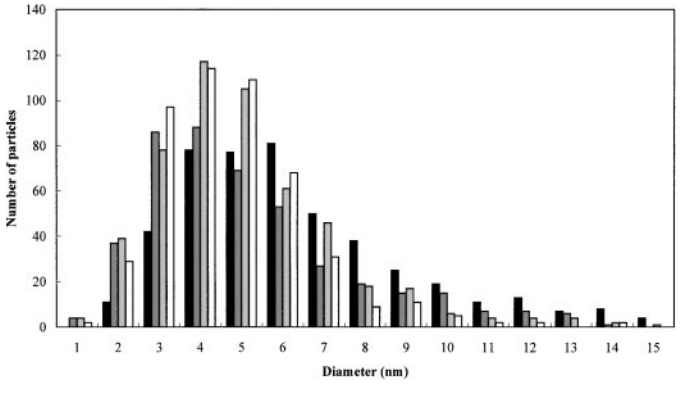

FIG. 4. Size distribution histograms of Pd–Pt clusters after reaction. Pure Pd (black), $Pd_{65}Pt_{35}$ (dark gray), $Pd_{17}Pt_{83}$ (light gray), and pure Pt (white).

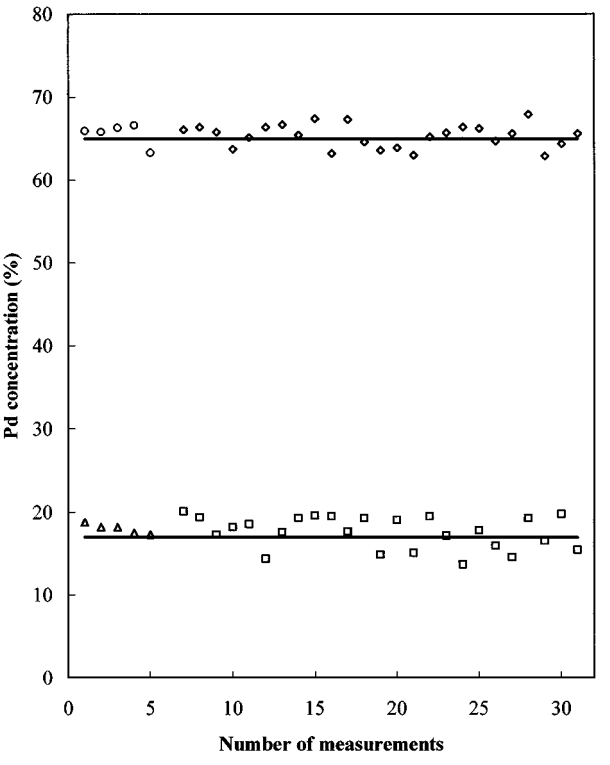

FIG. 5. Palladium concentration of a collection of alumina-supported $Pd_{65}Pt_{35}$ and $Pd_{17}Pt_{83}$ clusters. (△) and (○) correspond to large area whereas (◇) and (□) represent individual particles analysis.

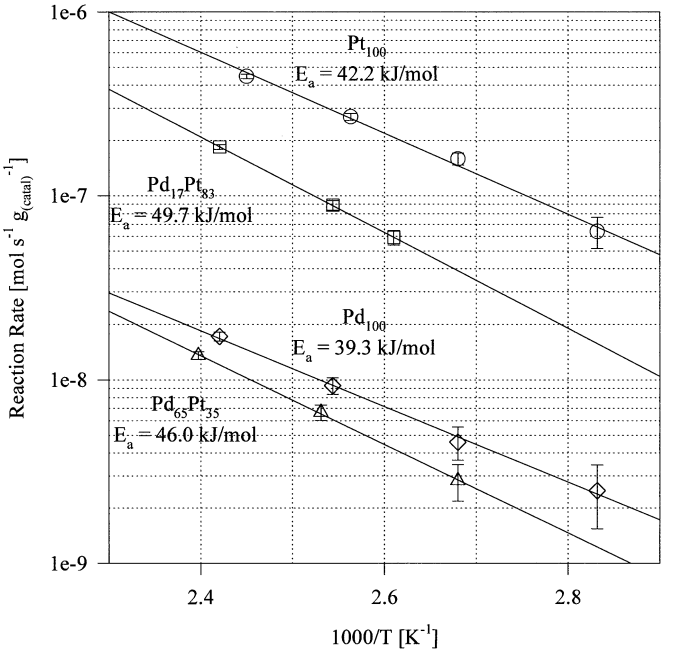

FIG. 6. Arrhenius plots for toluene hydrogenation over Pd–Pt catalysts at 740 Torr hydrogen and 20 Torr toluene. Pure Pd (◇), $Pd_{65}Pt_{35}$ (△), $Pd_{17}Pt_{83}$ (□), and pure Pt (○).

TABLE 2

Kinetics of Toluene Hydrogenation over Supported Pd–Pt Catalysts

Catalyst	Reaction order, toluene ($T = 393$ K)	Reaction order, H_2 ($T = 393$ K, $P_{toluene} = 18$ Torr)	Reaction order, toluene	Reaction order, H_2 ($P_{toluene} = 18$ Torr)	Activation energy (kJ/mol)	Maximum TOF ($s^{-1} \times 10^3$)
Pd	0.0	0.7	0.7 (533 K)	1.7 (533 K)	39.3	94
$Pd_{65}Pt_{35}$	0.0	0.5	0.3 (519 K)	1.6 (519 K)	46.0	133
$Pd_{17}Pt_{83}$	0.0	0.6	0.2 (498 K)	1.6 (498 K)	49.7	492
Pt	0.0	0.5	0.2 (488 K)	2.2 (488 K)	42.2	1800

histograms obtained after pretreatment and activity measurement of the catalysts.

Dependences of the reaction rate on toluene and hydrogen pressures are shown in Figs. 8 and 9 and the derived reaction orders are reported in Table 2. For each catalyst, the experiments were performed at temperatures below and above that of the maximum of activity (see Fig. 8). At low temperature, the reaction order with respect to H_2 is almost independent of the catalyst, with a mean value of 0.6 ± 0.1. At higher temperature, this reaction order increases to reach values ranging from 1.7 for pure Pd to 2.2 for pure Pt. The reaction order with respect to toluene is close to zero at low temperature and increases only slightly up to values ranging between 0.2 and 0.7 at higher temperature.

DISCUSSION

Determination of the Cluster Surface Compositions

The surface composition of alloys and especially the composition of the topmost surface layer are generally different from that of the bulk composition due to segregation processes (20). In a catalytic process, the reactants are adsorbed on the surface, implying that a first step in the understanding of the reactivity of alloys is the determination of the surface composition. The low-energy ion scattering technique is a surface-sensitive technique that selectively probes the outermost atomic layer. Generally, this technique is used to study bulk systems. Nevertheless, in a recent work (17), we have shown that LEIS can be applied to PdPt bimetallic clusters also produced by laser vaporization but deposited on flat supports. The main result is that the cluster surface is enriched with Pd for both alloys. More precisely, the Pd surface concentration reaches 38 and 87 at.% respectively for $Pd_{17}Pt_{83}$ and $Pd_{65}Pt_{35}$ alloys. In parallel with the LEIS

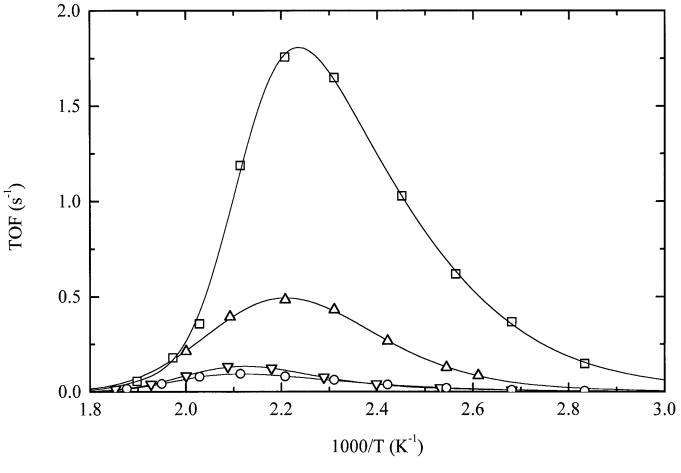

FIG. 7. Temperature effects on toluene hydrogenation over Pd–Pt catalysts. Pure Pd (○), $Pd_{65}Pt_{35}$ (▽), $Pd_{17}Pt_{83}$ (△), and pure Pt (□). The turnover frequencies (TOF) are based on microscopy experiments.

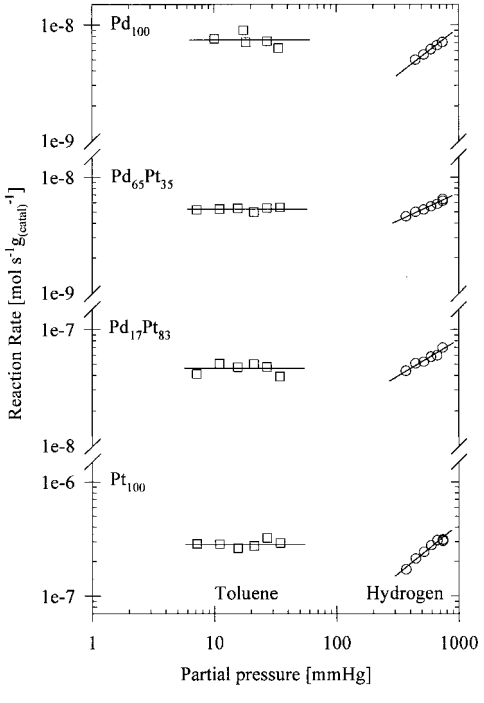

FIG. 8. Pressure dependencies of toluene hydrogenation on toluene and H_2 at $T = 393$ K over Pd–Pt catalysts.

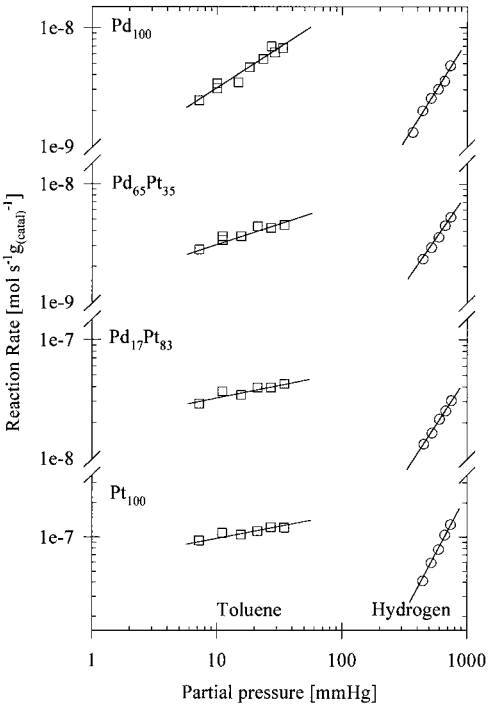

FIG. 9. Pressure dependencies on toluene and H_2 of toluene hydrogenation at high temperature over pure Pd (533 K), $Pd_{65}Pt_{35}$ (519 K), $Pd_{17}Pt_{83}$ (498 K), and pure Pt (488 K).

experiments, the modeling of the segregation process has been performed using Monte Carlo simulations (17). The deduced surface concentrations are in good agreement with experiments. Unfortunately, in the present case, we cannot use the LEIS results obtained previously since the annealing treatment gives rise to a mean size larger than that of the fresh catalyst and it is well known that surface segregation increases as the size increases because of the mass balance effect (the supply of atoms is limited for small particles). Moreover, in the present case, the metal loading is too low to measure by LEIS the surface composition with a reasonable accuracy. Nevertheless, we can predict the surface composition by using our theoretical model since it has been shown to give reliable results. The energetics model used has been thoroughly described elsewhere (20) and only the results will be presented in the present paper. The segregation behavior of Pd–Pt single-crystal alloys equilibrated at 600 K has been studied in this work and the first-layer composition has been calculated over the whole concentration range for the (111) and (100) orientations. For small particles, a large fraction of the atoms is located at the surface and the reservoir of diffusing atoms is thus limited by the total concentration of palladium. Therefore one has to correct the surface concentration determined for bulk alloys. The mass conservation implies that the surface and bulk concentrations (respectively X_S and X_B) *of a cluster* must verify the following equation:

$$X_N = DX_S + (1 - D)X_B \quad [1]$$

X_N is the nominal concentration (in the present case, 17 or 65%) and D is the calculated dispersion of the considered cluster assuming a truncated cubo-octahedral shape. For a given set of X_N and D, an infinity of (X_S, X_B) couples verify this equation but the actual X_S and X_B values must also satisfy the relation between surface and bulk composition corresponding to the thermodynamic equilibrium determined for a semi-infinite alloy (Fig. 10). Obviously, this unique couple of X_S and X_B values is given by the ordinate and the abscissa of the intersection of the straight line corresponding to Eq. [1], with the theoretical curves representing the surface composition of an equilibrated massive alloy. The results concerning the $Pd_{17}Pt_{83}$ alloy are displayed in Fig. 10 and summarized in Table 3. With the procedure described above, one calculates the surface Pd concentration and consequently the number of Pd surface atoms for each cluster size. Taking into account the size histogram of the $Pd_{17}Pt_{83}$ supported catalyst (Fig. 4) and weighting each class of size by the predicted surface number of Pd atoms for both (100) and (111) faces of the clusters (we have neglected corner and edge sites), one calculates a Pd surface concentration of 56%. Concerning the $Pd_{65}Pt_{35}$ alloy, the nominal Pd concentration is much higher and the calculations have shown that the surface is almost entirely covered by Pd atoms whatever the size of the clusters. This system illustrates the surface

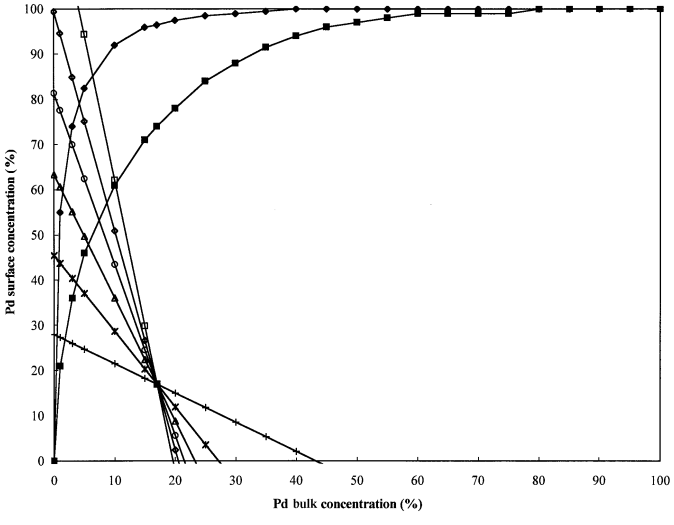

FIG. 10. Theoretical predictions for the Pd surface segregation versus Pd bulk concentration of $Pd_{17}Pt_{83}$ clusters. (◆) and (■) correspond respectively to bulk alloys with (100) and (111) orientations.The predicted surface compositions of the different faces of the clusters with different diameters d (assuming a cubo-octahedron shape) are determined by the intersects of the straight lines representing Eq. [1] with the curves corresponding to the bulk alloys. $d = 2$ nm (+), $d = 3.5$ nm (∗), $d = 5$ nm (△), $d = 6.5$ nm (○), $d = 8$ nm (◇), $d = 10.5$ nm (□).

TABLE 3

Segregation Statistics for $Pd_{17}Pt_{83}$ Clusters at $T = 600$ K

Truncated cubo-octahedron order	Particle size (nm)	Total number of atoms	Number of surface atoms	Surface Pd concentration (%) (100) faces	Surface Pd concentration (%) (111) faces	Surface Pd concentration (%)
3	1.8	201	122	30	27	27
5	3.4	1289	482	44	39	40
7	5.0	4033	1082	59	48	50
9	6.5	9201	1922	71	53	57
11	8.1	17561	3002	79	57	61
13	9.6	29881	4322	84	60	64
15	11.2	46929	5882	86	62	67
17	12.8	69473	7682	88	63	68
19	14.3	98281	9722	90	64	69

Note. For the sake of clarity, only odd cubo-octahedron orders have been presented but all orders have been taken into account for calculations of surface segregation.

behavior of a regular exothermic alloy with a low heat of mixing and it has been shown (20) that the large Pd surface segregation is associated with a Pd depletion in the second atomic layer.

Toluene Hydrogenation

A preliminary remark is that the turnover frequencies measured on our model Pt and Pd catalysts are consistent with the values reported in the literature (15, 16) for the activities of γ-Al_2O_3-supported Pd and Pt catalysts, prepared by the incipient wetness technique.

Secondly, as the Pd content increases, the TOF decreases and the maximum of activity shifts to higher temperature. This maximum occurs at T_{max} equal to 450, 456, 472, and 473 K on Pt, $Pd_{17}Pt_{83}$, $Pd_{65}Pt_{35}$, and Pd, respectively. Such a maximum has also been observed in the case of benzene (21, 22) and toluene (15, 22) hydrogenation over Pd and Pt supported catalysts. More precisely, in the case of benzene hydrogenation, a maximum of activity occurring at 473 K on Pt compared to 495 K on Pd (21) has been reported. This maximum is apparently not associated with thermodynamic equilibrium limitations, since the rate of the reverse reaction becomes appreciable only at higher temperature. This maximum has been explained by assuming either a decrease of the surface coverage by aromatics at high temperature (18) or the formation of hydrogen-deficient surface carbonaceous species resulting from a dehydrogenation of the aromatics (23). These hypotheses will be discussed later. A comparison of the results obtained with the four systems (Table 2) shows that the kinetics of toluene hydrogenation is rather similar on the pure metals and on the alloys. This similarity suggests that, at least for the rate-determining step, the same reaction mechanism occurs, even if the maximum activity of Pt is 19 times that of pure Pd. We also note that the activity curves of the pure Pd and $Pd_{65}Pt_{35}$ Catalysts are almost superimposed. However, even if the surfaces of both catalysts are entirely covered by Pd atoms, we have to keep in mind that for the $Pd_{65}Pt_{35}$ system, the Pd surface atoms are surrounded by Pt atoms located in the underlying layer. Hence, the nearly similar activities of these catalysts lead us to the conclusion that neighboring Pt atoms have no influence on the reactivity of Pd atoms. This rules out the assumption of electronic effects between these elements, as postulated by several authors (2, 24). The hydrogenation of toluene is considered to be structure insensitive, implying that the active site is composed of a small number of atoms. The effect of an inert or a slightly active diluent on the activity can be predicted, once the size of the active site has been determined.

To gain some insight into the structure of this site, one must first take into account the fact that these elements form a nearly regular solid solution, with a low heat of mixing and no ordered phase, over the whole concentration range (25). In this disordered system, the distribution of the atoms is simply governed by the statistics. Figure 11 displays the expected TOF at 400 K based on an ensemble of n Pd atoms or n Pt atoms and represented at a given temperature by

$$A = A_{Pd}X^n + A_{Pt}(1 - X)^n$$

where X is the palladium surface concentration and A_{Pd} and A_{Pt} are respectively the activities of pure Pd and Pt. This equation also implicitly assumes that mixed sites, which would have a reactivity different from that resulting from pure additivity of the elements, are not considered. The experimental activity of the $Pd_{17}Pt_{83}$ alloy follows a TOF versus Pd surface concentration curve corresponding to $n = 2$ atoms. Such an active-site size has been already postulated by Cadenhead and Masse (26), who studied benzene hydrogenation over Pd–Au alloy, whereas Leon and Vannice (27) determined a value of $n = 3$ for the benzene hydrogenation over Pd–Cu supported catalysts. One can also wonder if the active site can be described by two adjacent atoms over

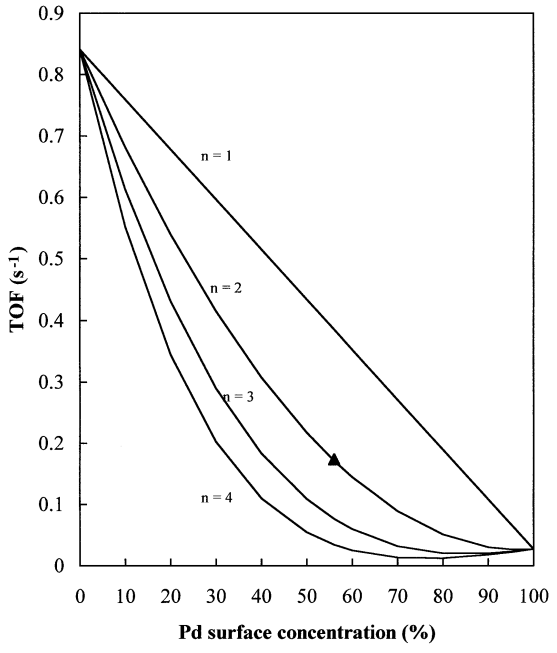

FIG. 11. Predicted dependence of turnover frequency on surface composition assuming that n Pd_s atoms or n Pt_s atoms constitute the active site. (▲) corresponds to the experimental value of the TOF at 400 K of the $Pd_{17}Pt_{83}$ catalyst assuming surface composition based on simulations.

the whole range of temperature. The activities of pure Pd, pure Pt, and $Pd_{17}Pt_{83}$ supported catalysts are presented in Fig. 12, with the expected activities assuming $n = 1$, $n = 2$, or $n = 3$ atoms. The comparison between the experiments and the simulations clearly shows, in the low-temperature range (up to 410 K), a perfect agreement for $n = 2$ atoms. However, as the temperature increases, a discrepancy arises and we even observe that the activity of the alloy becomes greater than that expected with $n = 1$. This paradoxical behavior should be related to the existence of a maximum in the activity (Fig. 7).

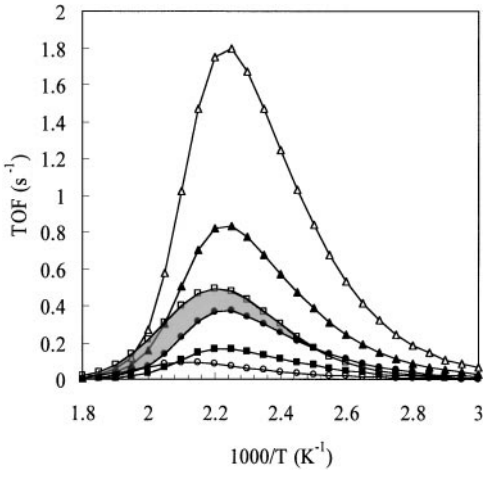

FIG. 12. Temperature dependence of the predicted turnover frequency (filled symbols) of the $Pd_{17}Pt_{83}$ catalyst assuming that n Pd_s atoms or $n$$Pt_s$ atoms constitute the active site. $n = 1$ (▲); $n = 2$ (●); $n = 3$ (■). Also shown are the activities (open symbols) of pure Pd catalyst (○), $Pd_{17}Pt_{83}$ (□), and pure Pt (△). The gray area represents the discrepancy between the predicted activity of the $Pd_{17}Pt_{83}$ catalyst assuming $n = 2$ and the activity determined experimentally.

Let us discuss this phenomenon on the basis of our knowledge on the adsorption properties of the reactants. First, in their comparative TDS study of the adsorption of benzene and toluene on Pt, Abon *et al.* (28) found a single and similar π adsorption mode for benzene and toluene, but with a much stronger bonding for the second molecule. Moreover, they observed that the adsorbed toluene is nearly completely dehydrogenated during the thermodesorption, whereas only half of the benzene desorbs dissociatively. Finally, they have also shown that toluene is thermally dehydrogenated 50 K below benzene. In spite of this difference, Orozco and Webb (22) in their study of the hydrogenation of a mixture of toluene and benzene on Pd/Al_2O_3 and Pt/Al_2O_3 found that, for both catalysts, the maximum in the activity–temperature curves is located at the same temperature for the two molecules.

All these observations suggest that the maxium in the activity curves cannot be related to the desorption or the dehydrogenation of the aromatics. Indeed, it would be difficult to understand how such aromatics with different adsorption properties would give rise to the same temperature maximum on both catalysts. So, one has to consider alternatively the possibility that this maximum is governed by the desorption of the hydrogen. If one compares the results of Conrad *et al.* (29) and Christmann *et al.* (30), who studied respectively the adsorption and desorption of H_2 on Pd and Pt single crystals, it should be noticed that the desorption peak of the hydrogen on Pd appears at a temperature slightly higher than on Pt. This agrees, at least qualitatively, with the fact that the maximum observed in the activity of Pd is located at a higher temperature than on Pt. Hence, in the course of the reaction at high temperature, the hydrogen could be supplied by the Pd on the alloy, the hydrogenation taking place to a large extent on Pt. This would explain the synergy between Pd and Pt observed at high temperature (Fig. 12) for $Pd_{17}Pt_{83}$, the only catalyst whose surface is composed of a mixed layer.

CONCLUSION

The laser vaporization technique has proven to be a unique way to obtain bimetallic clusters with a remarkably uniform composition. A simple explanation for this uniformity lies in the fact that the clusters are already formed before the deposition, whereas in chemical methods the composition is governed by the respective affinity of the precursors for the support. It constitutes a precious tool to investigate the effect of alloying on the reactivity,

independently of any possible support effect. Moreover, it is, in principle, adapted to obtain bimetallic catalysts with all kinds of alloys, even with nonmiscible metals like Au–Ni (19) or Ag–Ni (31). In the hydrogenation of toluene, the results concerning the pure metals are in agreement with those of the literature. On the bimetallic catalysts, we have demonstrated that no synergy between the two elements can be evidenced, the rates being perfectly explained by an additivity of the properties of the two metals. The nonlinear dependence of the rate as a function of the Pt surface concentration is interpreted by the presence of an adsorption site for the aromatic molecule composed of a pair of atoms.

Moreover, we have shown, with the study of the $Pd_{65}Pt_{35}$ sample, which contains nearly 100% Pd in the first layer, that the neighboring Pt atoms have no influence on the reactivity of Pd. This rules out the assumption of an electronic effect between these elements, a phenomenon postulated by several authors (2, 5, 24) but never demonstrated experimentally.

The behavior of the $Pd_{17}Pt_{83}$ bimetallic system at high temperature, which shows a cooperative effect between Pd and Pt, is interpreted by the ability of Pd to supply hydrogen in sufficient amount, whereas the aromatics remain more strongly bonded on platinum.

Finally, the possibility of obtaining well-tailored supported particles will be used in the near future to study in detail the resistance to sulfur poisoning of the Pd–Pt system as a function of the composition.

REFERENCES

1. Sinfelt, J. H., "Bimetallic Catalysts." Wiley, New York, 1983.
2. Koussathana, M., Vamvouka, D., Economou, H., and Verykios, X., *Appl. Catal.* **77**, 283 (1991).
3. Blomsma, E., Martens, J. A., and Jacobs, P. A., *J. Catal.* **165**, 241 (1997).
4. Carturan, G., Cocco, G., Facchin, G., and Navazio, G., *J. Mol. Catal.* **26**, 375 (1984).
5. Deganello, G., Duca, D., Liotta, L. F., Martorana, A., Venezia, A. M., Benedetti, A., and Fagherazzi, G., *J. Catal.* **151**, 125 (1995).
6. Jan, C., Lin, T., and Chang, J., *Ind. Eng. Chem. Res.* **35**, 3893 (1996).
7. Fujikawa, T., Idei, K., Ebihara, T., Mizuguchi, H., and Usui, K., *Appl. Catal. A* **192**, 253 (2000).
8. Yasuda, H., Matsubayashi, N., Sato, T., and Yoshimura, Y., *Catal. Lett.* **54**, 23 (1998).
9. Yasuda, H., Kameoka, T., Sato, T., Kijima, N., and Yoshimura, Y., *Appl. Catal.* **185**, 199 (1999).
10. Yasuda, H., and Yoshimura, Y., *Catal. Lett.* **46**, 43 (1997).
11. Cooper, B. H., and Donnis, B. B. L., *Appl. Catal. A* **137**, 203 (1996).
12. Kovach, S. M., and Wilson, G. D., U.S. Patent 3943053, Ashland Oil Inc., 1974.
13. Minderhoud, J. K., and Lucien, J. P., U.S. Patent 4960505, Shell Oil Co., 1988.
14. Winquist, B. H. C., Milam, S. N., Murray, B. D., and Ryan, R. C., EP Appl. 0519573, Shell IRM, 1992.
15. Rahaman, M. V., and Vannice, M. A., *J. Catal.* **127**, 251 (1991).
16. Lin, S. D., and Vannice, M. A., *J. Catal.* **143**, 554 (1993).
17. Rousset, J. L., Renouprez, A., and Cadrot, A. M., *Phys. Rev. B* **58**, 2150 (1998).
18. Chou, P., and Vannice, M. A., *J. Catal.* **107**, 129 (1987).
19. Rousset, J. L., Cadete Santos Aires, F. J., Sekhar, B. R., Mélinon, P., Prevel, B., and Pellarin, M., *J. Phys. Chem. B* **104**, 5430 (2000).
20. Rousset, J. L., Bertolini, J. C., and Miegge, P., *Phys. Rev. B* **53**, 4947 (1996).
21. Lin, S. D., and Vannice, M. A., *J. Catal.* **143**, 539 (1993).
22. Orozco, J. M., and Webb, G., *Appl. Catal.* **6**, 67 (1983).
23. Chou, P., and Vannice, M. A., *J. Catal.* **107**, 140 (1987).
24. Navarro, R. M., Pawelec, B., Trejo, J. M., Mariscal, R., and Fierro, J. L. G., *J. Catal.* **189**, 184 (2000).
25. Darby, J. B., and Myles, K. M., Jr., *Met. Trans.* **3**, 653 (1972).
26. Cadenhead, D. A., and Masse, N. G., *J. Phys. Chem.* **70**, 3558 (1996).
27. Leon y Leon, C. A., and Vannice, M. A., *Appl. Catal.* **69**, 305 (1991).
28. Abon, M., Bertolini, J. C., Billy, J., Massardier, J., and Tardy, B., *Surf. Sci.* **162**, 395 (1985).
29. Conrad, H., Ertl, G., and Latta, E. E., *Surf. Sci.* **41**, 435 (1974).
30. Christmann, K., Ertl, G., and Pignet, T., *Surf. Sci.* **54**, 365 (1976).
31. Rousset, J. L., *et al.*, to be published.